厚生労働科学研究費補助金（こころの健康科学事業）
（分担）研究報告書

α－ジストログリカノパチー候補タンパク質の評価方法の確立

分担研究者　野口　悟　国立精神・神経センター神経研究所室長

研究要旨　本研究では、生化学的に同定されたタンパク質遺伝子がα－ジストログリカノパチーの原因遺伝子候補となりうるかを評価するための解析方法の確立を目指した。培養筋細胞でのジストログリカン依存的なアセチルコリン受動体のクラスタリングを指標にした。ジストログリカンとフクチンsiRNA処理細胞ではそのクラスタリングの程度は小さくなっていた。

A. 研究目的

α-ジストログリカン（DG）の糖鎖修飾異常は、本邦に特異的に見られる福山型先天性筋ジストロフィー(FCMD)をはじめ、Walker-Warburg 症候群(WWS)、筋-眼-脳症候群(MEB)、先天性筋ジストロフィー(MDC) 1 D、MDC1c/LGMD2I など複数の重篤な筋ジストロフィーの病態と深く関わっている。これら疾患の責任遺伝子産物はいずれもα-DG の糖鎖修飾に関与すると考えられている。本事業で我々は、POMGnT1、フクチン、LARGE がゴルジ体シス領域に存在し、複合体を形成していること、FCMD 患者細胞で GlcNAc のα-DG への取り込みが起こらないことを示し、また、フクチン、LARGE の POMGnT1 機能への関与を示した。αDGP の約 20%の患者ではいまだ原因遺伝子が同定されておらず、他の遺伝子の関与が予想されている。我々は、POMGnT1、フクチン、LARGE 複合体に結合するタンパク質の同定を行うとともに、同定されたタンパク質遺伝子がαDGP の原因遺伝子候補となりうるのか、簡便な方法で評価できないかと考えた。培養基質に配向したラミニンを用いて培養された筋管細胞は、直径 10μm 程度の大きさの”Pretzel”と呼ばれるアセチルコリン受容体の集合体（クラスタリング構造）を形成する。アンチセンスオリゴを持ちいた研究から、このクラスタリング構造の形成はDG依存的であることが示されている。本研究では、このアセチルコリン受容体のクラスタリングを指標に、遺伝子のノックダウン法と組み合わせることで、αDGP の原因候補遺伝子の in vitro での評価が可能であるのかをモデル遺伝子系で調べた。これにより、DNA 配列解析の前段階としての簡便なα-DGP 原因遺伝子候補のスクリーニング法の確立を目指した。

B. 研究方法

培養細胞はマウス C2C12 細胞を用いた。培養基質として、ポリオルニチン添加ラミニンコートを用いた。筋管細胞への分化は定法に従い、血清を除去することで分化を誘導した。

DG及びフクチンsiRNAはInvitrogenから購入した。遺伝子ノックダウン効果はDGの発現レベルとフクチンのmRNA量により測定した。培養筋細胞への導入には Lipofectamine RNAiMAX 試薬（Invitrogen）を用いた。

アセチルコリン受容体の検出には TRITC

ラベルα-ブンガロトキシンを用いた。クラスタリングの測定は、オリンパス Fluoview 共焦点レーザー顕微鏡により行い、定量した。

（倫理面への配慮）

本研究において使用する全てのヒト検体は、国立精神・神経センター倫理委員会で承認された所定の承諾書を用いて、患者あるいはその親権者から遺伝子解析を含む研究使用に対する検体の使用許可（インフォームドコンセント）を得たものである。検体を使用するに当たっては、プライバシーを尊重し、匿名化した上で使用した。検体の保存ならびに匿名化したうえでの破棄は、患者および家族の意思を尊重している。遺伝子解析に関してはヒトゲノム解析研究に関する共通指針を遵守した。また、すべての動物実験は、国立精神・神経センター神経研究所動物実験に関する倫理指針に従い行った。研究に使用する際には、必要最小限度の動物を使用するとともに、動物に苦痛を与えないよう最大限の注意を払った。

C. 研究結果

DGおよびフクチンmRNAに対するそれぞれ2および3種のsiRNAを試した。 2種のDGsiRNA処理下でのβDG発現レベルは、未処理のコントロールに比べ、72及び11%の発現抑制が見られた。

培養筋管細胞は、基質に1型コラーゲンを用いた場合、長さが数μm程度の線状のアセチルコリン受容体の集合体を形成したが、配向したラミニンを用いて培養した場合、直径10μm程度の楕円状の”Pretzel”と呼ばれる集合体（クラスタリング構造）を形成した。

このPretzel構造は、DGおよびフクチンsiRNA処理によって、その数、面積ともに、明らかに減少した。未処理の筋管細胞では、単位面積あたり、45個のPretzelが観察されたが、DGsiRNA処理では、13-23個、フクチンsiRNA処理では、14-35個に減少していた。ひとつのPretzel構造の面積は、コントロールでは95±123μm^{2}であるのに対し、最も効果のあったDGsiRNA処理により40±23μm^{2}であった。また、最も効果のあった１種のフクチンsiRNA処理では74±101μm^{2}と減少を示した。他の２種ではPretzel数に減少がみられたものの、面積には変化が見られなかった。

D. 考察

今までのα-DGP 患者の検索では、約 20%の患者で、同定されている既知の原因遺伝子に変異が見られなかった。このことは、新たな原因遺伝子の可能性を示唆していた。さらに、我々は、昨年報告したフクチンを含む複合体への結合タンパク質を同定しているが、これが原因遺伝子である可能性を簡便に解析するシステムが必要であった。今回の方法ではっきりと、DG 遺伝子のノックダウン効果、またはDG 修飾タンパク質遺伝子のノックダウン効果を、筋管細胞でのアセチルコリン受容体のクラスタリングによって評価出来ることが出来た。この方法を用いれば、DNA の配列解析の前段階として、候補遺伝子を DG の機能解析を通して、絞り込むことが可能になると考えている。

E. 結論

培養筋細胞でのジストログリカン依存的なアセチルコリン受容体のクラスタリングを指標に、α－DGPの原因遺伝子候補を評価するための解析方法の確立を目指した。DGとフクチンsiRNA処理細胞ではクラスタリング度は小さくなっていた。

F. 健康危険情報

特になし

G. 研究発表

1．論文発表

Tanicguchi M, Kurahashi H, Noguchi S, Fukudome T, Okinaga T, Tsukahara T, Tajima Y, Ozono K, Nishino I, Nonaka I, Toda T: Aberrant neuromuscular junctions and delayed terminal muscle fiber maturation in α-dystroglycanopathies. *Hum Mol Genet* 15:1279-1289. 2006.

Wu S, Ibarra MCA, Malicdan MCV, Murayama K, Ichihara Y, Kikuchi H, Nonaka I, Noguchi S, Hayashi YK, Nishino I: Central core disease is due to RYR1 mutations in more than 90% of patients. *Brain* 129: 1470-1480, 2006.

Malicdan MC, Noguchi S, Nonaka I, Hayashi, YK, Nishino I: A Gne knockout mouse expressing human V572L mutation develops features similar to distal myopathy with rimmed vacuoles or hereditary inclusion body myopathy. *Hum Mol Genet* 16: 115-128, 2007.

Liewluck T, Hayashi YK, Osawa M, Kurokawa R, Fujita M, Noguchi S, Nonaka I, Nishino I: Unfolded protein response and aggresome formation in hereditary reducing body myopathy. *Muscle Nerve* 35:322-326, 2007.

Keira Y, Noguchi S, Kurokawa R, Fujita M, Minami N, Hayashi YK, Kato T, Nishino I: Characterization of lobulated fibers in limb girdle muscular dystrophy type 2A by gene expression profiling. *Neurosci Res* 57:513-521, 2007.

2．学会発表

村上てるみ，田辺雄三，松本浩，小川恵，埜中征哉，野口悟，林由起子，西野一三：フクチン遺伝子（FKTN）変異による多様な臨床病態．第47回日本神経学会総会，東京，5.11，2006.

西野一三, Wu Shiwen, Ibarra Carlos, Malicdan May，村山久美子，埜中征哉，野口悟，林由起子:セントラルコア病の大半はRYR1変異による．第47回日本神経学会総会，東京，5.11，2006.

Malicdan May，野口 悟，林由起子，埜中征哉，西野一三：縁取り空胞を伴う遠位型ミオパチー（DMRV）のモデルマウス作製．第47回日本神経学会総会，東京; 5.12，2006.

村上てるみ，田辺雄三，埜中征哉，小川 恵，野口 悟，林由起子，大澤真木子，西野一三：肢帯型筋ジストロフィー2L 型？ FKTN 遺伝子異常の最軽症例．第23回小児神経筋疾患懇話会．東京，8.19，2006.

Nishino I, Wu S, Ibarra C, Malicdan M, Murayama K, Noguchi S, Hayashi YK, Nonaka I: Central Core Disease Is Due to RYR1 Mutations in More Than 90% of Patients. 58th Annual Meeting of American Academy of Neurology. San Diego, CA, USA. 4.5, 2006.

Noguchi S, Ogawa M, Murayama K, Matsumoto H, Imamura M, Hayashi YK, Nishino I: Fukutin and LARGE Cooperatively work with POMGnT1 on N-acetylglucosamine transfer in *O*-mannosylglycan synthesis of alpha-dystroglycan. XIth International Congress on Neuromuscular Diseases. Istanbul, Turkey, 3 July 2006.

Astejada M, Hayasi YK, Fujita M, Uematsu F, Nonaka I, Noguchi S, Nishino I: Disruption of the in vivo regeneration process in cardiotoxin-injected Emdy/-Mice. XIth International Congress on Neuromuscular Diseases. Istanbul, Turkey, 3 July 2006.

Keira Y, Kurokawa R, Fujita M, Minami N, Hayashi YK, Noguchi S, Kato T, Nishino I: Gene expression of Limb girdle muscular

dystrophy type 2A. XIth International Congress on Neuromuscular Diseases. Istanbul, Turkey, 3 July 2006.

Murakami T, Tanabe Y, Ogawa M, Nonaka I, Noguchi S, Hayashi YK, Nishino I: Fukutin (FKTN) mutations can cause cardiomyopahty. XIth International Congress on Neuromuscular Diseases. Istanbul, Turkey, 3 July 2006.

Hayashi YK, Goto K, Nagano A, Ura S, Kawahara G, Astejada M, Nonaka I, Noguchi S, Nishino I: Emerinopathy and laminopathy in Japan. XIth International Congress on Neuromuscular Diseases. Istanbul, Turkey, 3 July 2006.

Kawahara G, Okada M, Morone N, Ibarra MCA, Nonaka I, Noguchi S, Hayashi YK, Nishino I: A heterozygous COL6A1 glycine substitution that influences cell attachment in fibroblasts causes sarcolemma-specific collagen VI deficiency(SSCD). XIth International Congress on Neuromuscular Diseases. Istanbul, Turkey, 3 July 2006.

Okada M, Kawahara G, Nonaka I, Noguchi S, Hayashi YK, Nishino I: Collagen VI deficiency is the second leading cause of congenital muscular dystrophy in Japan. XIth International Congress on Neuromuscular Diseases. Istanbul, Turkey, 3 July 2006.

Malicdan MCV, Noguchi S, Hayashi YK, Nonaka I, Nishino I: A GNE knockout mouse expressing human V572L mutation develops features similar to distal myopathy with rimmed vacuoles(DMRV). XIth International Congress on Neuromuscular Diseases. Istanbul, Turkey, 4 July 2006.

Sato I, Ibarra MCA, Wu S, Noguchi S, Hayashi YK, Nonaka I, Nishino I: RYR1 mutation in congenital neuromuscular disease with uniform type 1 fiber. XIth International Congress on Neuromuscular Diseases. Istanbul, Turkey, 4 July 2006.

Ohkuma A, Murayama K, Ogawa M, Noguchi S, Hayashi YK, Nonaka I, Nishino I: The genetic cause of lipid storage myopathy is unknown in more than 80% of the cases. XIth International Congress on Neuromuscular Diseases. Istanbul, Turkey, 4 July 2006.

Ibarra MCA, Malicdan MCV, Wu S, Murayama K, Ichihara Y, Kikuchi H, Noguchi S, Hayashi YK, Nonaka I, Nishino I: Pathlogical findings in muscle from malignant hyperthermiasusceptible patints. XIth International Congress on Neuromuscular Diseases. Istanbul, Turkey, 6 July 2006.

Arahata H, Fujita M, Murayama K, Ogawa M, Noguchi S, Hayashi YK, Raheem O, Udd B, Nishino I: The identification of non-DM1, non-DM2 Patient in clinical DM patients. XIth International Congress on Neuromuscular Diseases. Istanbul, Turkey, 6 July 2006.

Noguchi S, Fujita M, Sasaoka T, Nishino I: The therapeutic effect of myostatin-blockade on muscular dystrophic mice and gene expression analysis of the treated muscles. 11th International Congress of the World Muscle Society. Bruges, Belgium, 6 October 2006.

Hayashi YK, Astejada MN, Ozawa R, Fujita M, Noguchi S, Nonaka I, Stewart CL, Nishino I: Three kinds of model mice for nuclear envelopathy. 11th International Congress of the World Muscle Society. Bruges, Belgium, 5 October 2006.

Malicdan MC, Noguchi S, Hayashi YK, Nonaka I, Nishino I: A GNE knockout mouse expressing human V572L mutation develops features similar to Nonaka myopathy or distal myopathy with rimmed vacuoles (DMRV). 11th International Congress of the World Muscle Society. Bruges, Belgium, 4 October 2006.

Murakami T, Hayashi YK, Noguchi S, Nonaka I, Campbell KP, Osawa M, Nishino I: Fukutin gene mutations can cause familial dilated cardiomyopathy with minimal muscle weakness and normal intellience. The 9th Asian & Oceanian Congress of Child Neurology. Cebu Philippine, 24 Jan 2007.

H. 知的財産権の出願・登録状況（予定を含む）

1．　特許取得

特になし

2．　実用新案登録

特になし

3．　その他

特になし

Ⅲ.　研究成果の刊行に関する一覧表

研究成果の刊行に関する一覧表

発表者氏名： 論文タイトル名. 発表誌名 巻号： ページ, 出版年
Goto K, Nishino I, Hayashi YK: Rapid and accurate diagnosis of facioscapulohumeral muscular dystrophy. ***Neuromuscul Disord*** 16:256-261. 2006.
Taniguchi M, Kurahashi H, Noguchi S, Fukudome T, Okinaga T, Tsukahara T, Tajima Y, Ozono K, Nishino I, Nonaka I, Toda T: Aberrant neuromuscular junctions and delayed terminal muscle fiber maturation in α-dystroglycanopathies. ***Hum Mol Genet*** 15:1279-1289. 2006.
Wu S, Ibarra MCA, Malicdan MCV, Murayama K, Ichihara Y, Kikuchi H, Nonaka I, Noguchi S, Hayashi YK, Nishino I: Central core disease is due to RYR1 mutations in more than 90% of patients. ***Brain*** 129: 1470-1480, 2006.
Malicdan MC, Noguchi S, Nonaka I, Hayashi YK, Nishino I: A Gne knockout mouse expressing human V572L mutation develops features similar to distal myopathy with rimmed vacuoles or hereditary inclusion body myopathy. ***Hum Mol Genet*** 16: 115-128, 2007.
Osawa M, Liewluck T, Ogata K, Iizuka T, Hayashi YK, Nonaka I, Sasaki M, Nishino I: Familial reducing body myopathy. ***Brain Dev*** 29: 112-116, 2007.
Liewluck T, Hayashi YK, Osawa M, Kurokawa R, Fujita M, Noguchi S, Nonaka I, Nishino I: Unfolded protein response and aggresome formation in hereditary reducing body myopathy. ***Muscle Nerve*** 35:322-326, 2007.
Keira Y, Noguchi S, Kurokawa R, Fujita M, Minami N, Hayashi YK, Kato T, Nishino I: Characterization of lobulated fibers in limb girdle muscular dystrophy type 2A by gene expression profiling. ***Neurosci Res*** 57:513-521, 2007.

Ⅳ.　研究成果の刊行物・別刷

PERGAMON

Neuromuscular Disorders 16 (2006) 256–261

www.elsevier.com/locate/nmd

Rapid and accurate diagnosis of facioscapulohumeral muscular dystrophy

Kanako Goto, Ichizo Nishino, Yukiko K. Hayashi *

Department of Neuromuscular Research, National Institute of Neuroscience, National Center of Neurology and Psychiatry (NCNP), 4-1-1 Ogawa-Higashi, Kodaira, Tokyo 187-8502, Japan

Received 10 September 2005; received in revised form 9 January 2006; accepted 18 January 2006

Abstract

Facioscapulohumeral muscular dystrophy (FSHD) is a common muscular disorder, but clinical and genetic complications make its diagnosis difficult. Southern blot analysis detects a smaller sized *Eco*RI fragment on chromosome 4q35 in most facioscapulohumeral muscular dystrophy patients, that contains integral number of 3.3-kb tandem repeats known as D4Z4. The problems for the genetic diagnosis are that southern blotting for facioscapulohumeral muscular dystrophy is quite laborious and time-consuming, and the D4Z4 number is only estimated from the size of the fragment. We developed a more simplified diagnostic method using a long polymerase chain reaction (PCR) amplification technique. Successful amplification was achieved in all facioscapulohumeral muscular dystrophy patients with an *Eco*RI fragment size ranging from 10 to 25 kb, and each patient had a specific polymerase chain reaction product which corresponded to the size calculated from the number of D4Z4. Using southern blot analysis, more than 90% of facioscapulohumeral muscular dystrophy patients have a smaller *Eco*RI fragment than 26 kb in our series, and the number of D4Z4 repeats is precisely counted by this polymerase chain reaction method. We conclude that this long polymerase chain reaction method can be used as an accurate genetic screening technique for facioscapulohumeral muscular dystrophy patients.

Keywords: Facioscapulohumeral muscular dystrophy; Chromosome 4q35; Genetic diagnosis; Southern blotting; PCR; *Eco*RI fragment; D4Z4

1. Introduction

Facioscapulohumeral muscular dystrophy (FSHD) is a common autosomal dominant muscular disorder characterized by its distinct clinical presentation. It often involves weakness and atrophy of facial muscles, followed by shoulder-girdle, the scapula fixators, and the upper arm muscles. Subsequently, pelvic girdle and lower limbs are also affected. About 20% of the patients eventually become wheelchair-bound by 40 years of age [1]. Difficulties of whistling, eye closure, or arm raising are common initial symptoms. Prominent scapular winging and horizontally positioned clavicles are also observed. Facial or shoulder girdle weakness usually appears during adolescence, but signs may be apparent on examination even in early childhood. Asymmetry of muscle involvement is often observed in apparently affected patients, but this is unrelated to handedness [2]. Weakness is relatively mild and the progression is usually slow with frequent association of subclinical hearing loss and retinal vasculopathy. The clinical diagnosis of FSHD is sometimes difficult because the onset of illness and the phenotypic expression is extremely variable, both within and between families [3,4].

The gene locus for FSHD has been identified on chromosome 4q35 wherein an array of tandem repeat units is located. Each repeat is a 3.3-kb *Kpn*I digestable fragment designated as D4Z4 (Fig. 1) [5–7]. The disease is usually associated with a deletion of this repeated region, however the responsible gene has not yet been identified, and the underlying molecular mechanism is still enigmatic. Southern blot analysis using the probe p13E-11 (D4F104S1) [6] is usually performed in the genetic diagnosis of FSHD. Normal individuals have *Eco*RI digested fragments containing D4Z4 repeats which varies from 40 kb to more than 300 kb in size, however, most of the FSHD patients have a smaller sized fragment from 10 to 35 kb. The clinical severity is often correlated to the fragment size, and patients with the smallest *Eco*RI fragment show very early onset and can be associated with epilepsy and mental retardation [8,9].

* Corresponding author. Tel.: +81 42 341 2712; fax: +81 42 346 1742.
E-mail address: hayasi_y@ncnp.go.jp (Y.K. Hayashi).

0960-8966/$ - see front matter © 2006 Elsevier B.V. All rights reserved.
doi:10.1016/j.nmd.2006.01.008

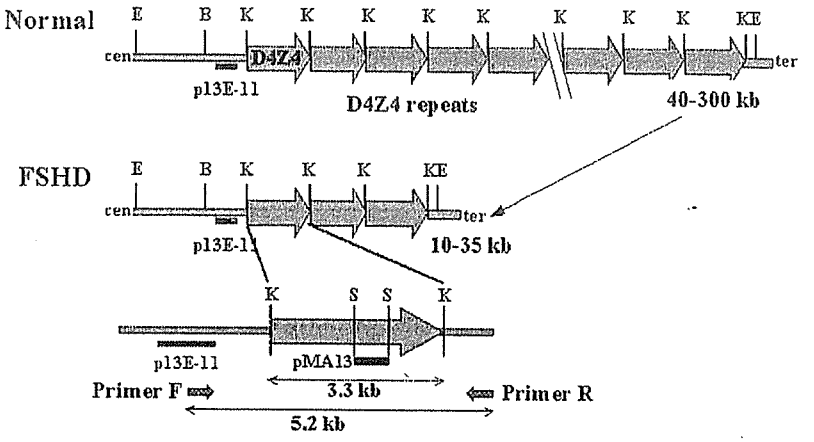

Fig. 1. A schematic diagram of the FSHD gene region on chromosome 4q35 showing the relative locations of primers and the probes used in this study. The primer set has been designed in the non-repeated region, and is expected to produce a 5.2 kb PCR amplified product when template genomic DNA contains one D4Z4 repeat. Cen, centromeric side of the gene; ter, telomeric side of gene; E, *Eco*RI; B, *Bln*I; K, *Kpn*I; S, *Sal*I.

Presently, the accuracy of the molecular diagnosis for FHSD using southern blot is up to 98% [10], however, several factors make this method cumbersome, and more than a week-length of time is required to obtain the results. In the conventional southern blotting method, it is difficult to resolve fragment size over 50 kb, and pulsed-field gel electrophoresis (PFGE) is sometimes taken together to increase resolution. Somatic and germline mosaicism is frequently observed in which more than three different sized *Eco*RI fragments on chromosome 4q are identified [11,12]. Furthermore, homologous 3.3-kb repeat-like sequences are also identified on many other chromosomes such as chromosomes Y and 3p [13,14]. In addition, chromosome 10q26 also contains 3.3-kb *Kpn*I digestable tandem repeats with 98% nucleotide identity to D4Z4 on chromosome 4 [15,16]. Consequently, there is a high incidence of inter-chromosomal exchange between 4q35 and 10q26, which is observed in about 20% of normal individuals [17,18]. In southern blot analysis, the probe p13E-11 used is not specific only to recognize *Eco*RI fragment from chromosome 4q but can also identify *Eco*RI fragment on chromosomes 10q26 and Y. This would require double restriction enzyme digestion using *Eco*RI and *Bln*I to be performed to distinguish 4q35-derived D4Z4 (*Bln*I-resistant) from 10q26-derived repeated units (*Bln*I-sensitive) [19]. From these complexities, there is an urgent need to develop a more simplified and reliable method for the diagnosis of FSHD.

Here, we introduce a new method to count the numbers of D4Z4 repeats on chromosome 4q35 by using long PCR amplification, which is quite useful for the rapid and accurate genetic diagnosis of FSHD.

2. Materials and methods

All clinical materials used in this study were acquired with informed consent. One hundred and five patients with a 4q-linked small *Eco*RI fragment from 10 to 35 kb (Table 3), and seven healthy individuals were examined. Genomic DNA was carefully and gently extracted from blood lymphocytes using a standard method. Southern blot analysis using the probe p13E-11 was performed as previously described [12].

For a long PCR amplification, a 50 μl reaction mixture was used. This mixture contains 400–600 ng of genomic DNA, 25 μl of 2× GC Buffer I (TAKARA BIO INC. Japan), 7.5 μl dATP/dTTP/dCTP mixture (10 mM each), 2.5 μl dGTP/7-deaza-dGTP mix (2:3), 1 μl (10 pM/μl) of each primers, and 0.5 μl (5 U/μl) LA Taq HS (TAKARA BIO). The primers were designed based on the human genomic sequences from GenBank (Accession Numbers D38025 and U74497). The primer sequences are F: 3′-GGCCAGAGTTT-GAATATACTGTGGTCATCTCTGCTCCAG-5′, R: 3′-CAGGGGATATTGTGACATATCTCTGCACTCATC. Amplification was performed using GeneAmp PCR System 9700 (PerkinElmer Japan Co., Ltd, Japan) with the following conditions; 1 min at 94 °C for the initial denaturation, followed by 10 cycles of 10 s at 98 °C and 20 min at 64 °C, and an additional 23 cycles of 10 s at 98 °C, 20 min with autoextension of 20 s per cycle at 64 °C, and 10 min at 72 °C for final elongation. The PCR products were separated by electrophoresis using 0.4% SeaKem HGT agarose gel (FMC BioProducts, ME) in 1× TAE with 0.5 μg/ml ethidium bromide at 3 h. High Molecular Weight DNA Marker (8.3–48.5 kb) (Invitrogen Japan K.K., Japan) and 1 kb plus ladder (Invitrogen) were used. The number of the 3.3 kb *Kpn*I repeated units in the FSHD gene region was calculated by the sequence data from GenBank (Accession Numbers D38024, D38025, and U74497).

In order to ascertain the specificity of the amplified products, we transferred the gels to Hybond N^+ (Amersham Biosciences, Japan) and overnight hybridization at 65 °C was performed with the ^{32}P-labeled probes of p13E-11 and pMA13 (1.3 kb *Stu*I fragment within a D4Z4 unit). The membrane was washed in a stringency of 2× SSC/0.1% SDS for 20 min at 65 °C for two times, followed by

Table 1
Comparison of long PCR and southern blot (SB) analyses

	PCR	SB
Template DNA (μg)	0.4	40
Enzyme digestion	No	*Eco*RI, *Bln*I
Gel size, concentration	11×14 cm, 0.4%	20×20 cm, 0.3%
Required time (h)		
PCR	11	0
Electrophoresis	3	68
Transfer	0	18
Hybridization	0	18
Detection	EB	RI
Total time required	<1 day	7–10 days
Accuracy (%)	90.1[a]	98 [10]

EB, ethidium bromide; RI, radio isotope.
[a] Estimated from the distribution of *Eco*RI fragment size in our series as described in Table 2.

autoradiography for 2 h using BAS2500 image analyzer (Fiji Photo Film, Japan).

3. Results

Table 1 shows the comparison of our newly developed long PCR method and the conventional southern blot analysis. This long PCR method is quite simple, requiring only a small amount of genomic DNA (1/100 of the quantity for southern blotting) and results are rapidly acquired overnight.

The long PCR method amplified five different sized products of 5.2, 8.5, 11.8, 15.1 and 18.4 kb which corresponded to the calculated size from the sequence data of the FSHD region containing one to five D4Z4 repeats, respectively (Fig. 2a, Table 3). These PCR products were not digested by *Bln*I, and were exclusively hybridized by the two probes of p13E-11 and pMA13 (data not shown). The same PCR method was performed on 10 individuals with a small *Eco*RI fragment (from 10 to 25 kb) on chromosome 10q26 but no amplified product was identified (data not shown).

Table 2 shows the distribution of the size of small *Eco*RI fragment on chromosome 4q of 263 FSHD families in our series. Table 3 shows the size of the PCR products, the calculated size of the *Eco*RI fragment, the range of the fragment size detected by southern blot analysis, and number of the patients. A 5.2 kb PCR product that contains one D4Z4 repeat was observed in eight patients with a *Eco*RI fragment from 10 to 11 kb. Sequence analysis confirmed that this 5.2 kb fragment contains one D4Z4 repeat on chromosome 4q35. An 8.5 kb band corresponding to the size with two D4Z4 repeated units was detected in 23 patients with 13–17 kb *Eco*RI fragment. An 11.8 kb product (three D4Z4 repeats) was seen in 26 patients with 16–19 kb fragment, a 15.1 kb fragment (four D4Z4 repeats) was seen in 24 patients with 18–22 kb fragment, and a 18.4 kb product (five D4Z4 repeats) was observed in six patients with 23–25 kb *Eco*RI fragment. The PCR products were amplified from all 87 DNA samples of the patients with an *Eco*RI fragment of 25 kb or less. However, DNA from normal individuals and FSHD patients with larger (≧26 kb) *Eco*RI fragments were not successfully amplified/detected by this long PCR method.

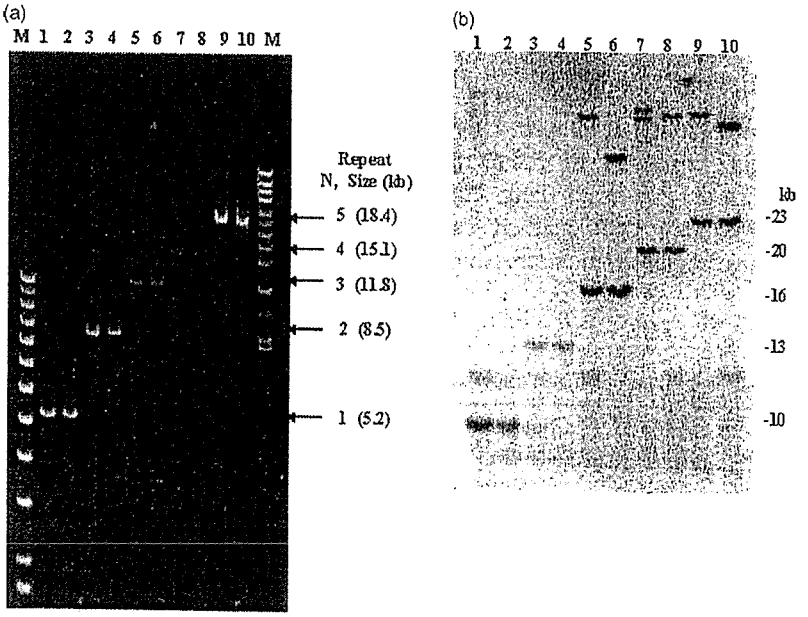

Fig. 2. Long PCR amplification and conventional southern blot analysis using genomic DNA from FHSD patients. (a) A 5.2 kb PCR product was detected on two patients with an *Eco*RI fragment of 10-kb (lane 1), or 11-kb (lane 2) as interpreted from our previous southern blot study. An 8.5-kb band was detected from two patients with a 13-kb (lane 3) or a 14-kb (lane 4) fragment, an 11.8-kb product from two patients with a 16-kb (lane 6) or a 17-kb (lane 7) fragment, a 15.1-kb product from a 20 or a 22 kb fragment, and an 18.4 kb fragment was identified from patients with a 24 and a 25 kb *Eco*RI fragment. These PCR products correspond to the size containing one to five D4Z4 repeated units. (b) Southern blot analysis using the same 10 samples in (a). The samples with the same size of the PCR products showed no difference of the *Eco*RI fragment size, although variable fragment size was previously interpreted.

Table 2
Distribution of *Eco*RI fragment size on chromosome 4q of 263 families in our series

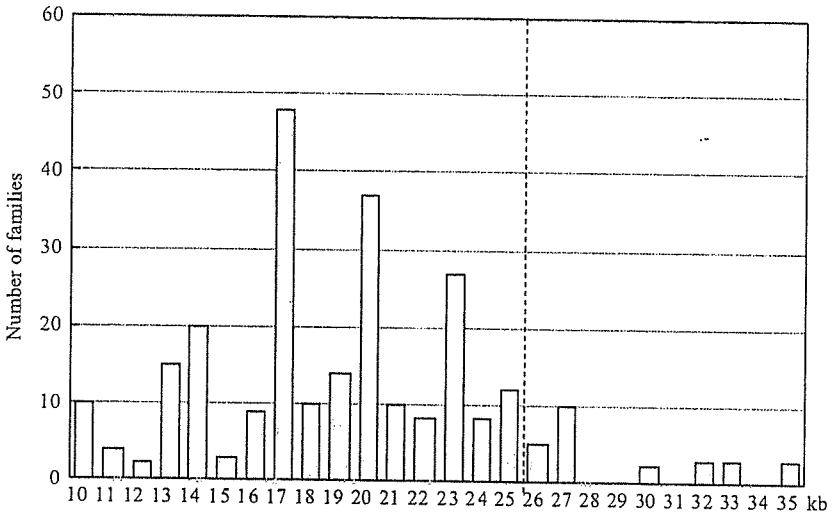

*Eco*RI fragments of <26 kb (dot line) can be amplified by long PCR analysis.

Estimated fragment size from the previous southern blot was not identical among the patients with same numbers of D4Z4 repeats. To determine the inter-individual variability of the fragment size, conventional southern blot analysis was repeated simultaneously. Notably, after the repeated southern blot technique, the *Eco*RI fragment size was similar when the D4Z4 number was the same and this result was consistent with the calculated size (Fig. 2b).

4. Discussions

In this study, we have successfully developed a new method for rapid and specific diagnosis of FSHD by counting the number of D4Z4 repeats via a long PCR amplification technique. This long PCR method can specifically amplify the repeated region from chromosome 4q up to 18.4 kb in size and countable from one to five D4Z4 repeated units.

Table 3
Comparison of the results of long PCR and southern blot (SB) analysis

Number of D4Z4 repeats	PCR product size (kb)	Calculated size of *Eco*RI fragment (kb)	Range of *Eco*RI fragment by SB (kb)	Number of patients examined by PCR
1	5.2	10.2	10-11	8
2	8.5	13.5	13–17	23
3	11.8	16.8	16–19	26
4	15.1	20.1	18–22	24
5	18.4	23.4	23–25	6
6	21.7	26.7	26–35	18 (No amplification)
7	25	30		
8	28.3	33.3		
9	31.6	36.6		

D4Z4 repeat has highly GC-rich sequence up to 73% [20]. Difficulties in PCR amplification often arise when GC content of the template DNA exceeds 50%. This difficulty in PCR amplification was overcame in our study by using thermo-stable long accurate Taq, 7-deaza-dGTP, and a higher denaturing temperature (98 °C) followed by a relatively higher annealing/extension temperature (64 °C) for 20 min with autoextension of 20 s per cycle. Therefore 73% of GC-containing repeated region of more than 18 kb in size was amplified with ease. The specificity of each PCR amplified product was ascertained by several ways. First, both probes (p13E-11 and pMA-13) that were used in the hybridization of the PCR products exclusively recognize fragments containing D4Z4 repeats. Second, the restriction enzyme *Bln*I did not digest the amplified fragments and confirmed that the product is apparently different from the repeats derived from chromosome 10q26, wherein 98% homologous *Kpn*I repeated units and franking sequences are known. Third, this long PCR method did not amplify *Kpn*I repeats from 10q26 even though the only difference is one different nucleotide from each of the primer region on 4q35. We also designed 10q-specific primer set and confirmed that only the 10q-derived repeats could be amplified by using this primer set.

The diagnosis of FSHD is sometimes difficult. Clinical symptoms and severity are quite variable between the patients even within the same family. Up to date, genetic diagnosis of FSHD is solely depended on the southern blot analysis since no responsible gene is yet identified within the candidate region. However, such procedure requires a large amount of DNA and would necessitate at least a week-time period to produce results. The requirement for such

amount of time for analysis dwells on the complexity of the experimental protocols in detecting the various fragments, the sizes ranging from 10 to 300 kb, as well as the determination of the existence of homologous regions on the other chromosomes. Determination of the size of *Eco*RI fragment is important since it is usually correlated to the clinical severity. However, identification of the precise fragment size is often difficult in the conventional southern blotting, since only very low concentrated gels of 0.3% is used to detect large sized fragment, and even minor changes in the experimental conditions would produce different results. In fact, in our very own series, DNA samples containing the same number of D4Z4 repeats showed the same *Eco*RI fragment size on one membrane although the estimated size in our previous analysis detected by different membranes were variable. Therefore, the number of D4Z4 units estimated from the *Eco*RI fragment size using Southern blotting could be misinterpreted from its actual number. From the result of the long PCR analysis, we concluded that the number of D4Z4 is countable from the size of PCR products, and the deletion of the FSHD region is certainly caused by the deleted integral number of D4Z4.

The number of D4Z4 is specifically countable up to five, which corresponds to the estimated *Eco*RI fragment of 10–25 kb in size. When no amplified product was obtained, southern blot analysis is required. In our series, 9.9% of the 4q-linked small *Eco*RI fragments have 26–35 kb as shown in Table 2, but the percentage may be greater in other countries. In the cases having deletion of p13E-11, no product can be obtained in this PCR analysis, since the forward primer is designed within this region. However, considering the complexity of the southern blot technique, this long PCR analysis is useful for the initial screening of the FSHD patients, and also the genetic test for the other family members with a known D4Z4 repeat numbers from 1 to 5 in an index patient. Obtaining accurate results rapidly is always beneficial for the patient, especially during prenatal test. From the economical point of view, PCR analysis is also beneficial since it costs 1/30–40 for the southern blot analysis.

Both primer sequences we used in this study are 4q-specific, and can amplify fragments even those with zero D4Z4 repeat, if any, producing an estimated 1.9-kb product. We also designed a primer set that can specifically amplify the repeated region on chromosome 10q. Theoretically, by using several combinations of these primers, we should be able to distinguish rare cases with short hybrid repeats on 4q or non-FSHD *Bln*I-resistant fragments on 10q. We concluded that the long PCR method could be used as an accurate genetic screening technique for FSHD.

Acknowledgements

We would like to thank Dr Mina Nolasco Astejada (NCNP) for critically reviewing the manuscript. This work was supported by Health and Labor Science Research Grants, Research on Psychiatric and Neurological Diseases and Mental Health, and The Research Grant (17A-10) for Nervous and Mental Disorders from the Ministry of Health, Labour and Welfare, Research on Health Sciences focusing on Drug Innovation from The Japan Health Sciences Foundation, Japan.

References

[1] Lunt PW, Harper PS. Genetic counselling in facioscapulohumeral muscular dystrophy. J Med Genet 1991;28:655–64.
[2] Tawil R, McDermott MP, Mendell JR, Kissel J, Griggs RC. Facioscapulohumeral muscular dystrophy (FSHD): design of natural history study and results of baseline testing, FSH-DY group. Neurology 1994;44:442–6.
[3] Lunt PW, Jardine PE, Koch M, et al. Phenotypic–genotypic correlation will assist genetic counseling in 4q35-facioscapulohumeral muscular dystrophy. Muscle Nerve 1995;2:S103–S9.
[4] Padberg GW, Frants RR, Brouwer OF, Wijmenga C, Bakker E, Sandkuijl LA. Facioscapulohumeral muscular dystrophy in the Dutch population. Muscle Nerve 1995;2:S81–S4.
[5] Upadhyaya M, Lunt P, Sarfarazi M, Broadhead W, Farnham J, Harper PS. The mapping of chromosome 4q markers in relation to facioscapulohumeral muscular dystrophy (FSHD). Am J Hum Genet 1992;51:404–10.
[6] Wijmenga C, Hewitt JE, Sandkuijl LA, et al. Chromosome 4q DNA rearrangements associated with facioscapulohumeral muscular dystrophy. Nat Genet 1992;2:26–30.
[7] Hewitt JE, Lyle R, Clark LN, et al. Analysis of the tandem repeat locus D4Z4 associated with facioscapulohumeral muscular dystrophy. Hum Mol Genet 1994;3:1287–95.
[8] Funakoshi M, Goto K, Arahata K. Epilepsy and mental retardation in a subset of early onset 4q35-facioscapulohumeral muscular dystrophy. Neurology 1998;50:1791–4.
[9] Miura K, Kumagai T, Matsumoto A, et al. Two cases of chromosome 4q35-linked early onset facioscapulohumeral muscular dystrophy with mental retardation and epilepsy. Neuropediatrics 1998;29: 239–41.
[10] Upadhyaya M, Cooper DN. Molecular diagnosis of facioscapulohumeral muscular dystrophy. Expert Rev Mol Diagn 2002;2: 160–71.
[11] Lemmers RJ, van der Wielen MJ, Bakker E, Padberg GW, Frants RR, van der Maarel SM. Somatic mosaicism in FSHD often goes undetected. Ann Neurol 2004;55:845–50.
[12] Goto K, Nishino I, Hayashi YK. Very low penetrance in 85 Japanese families with facioscapulohumeral muscular dystrophy 1A. J Med Genet 2004;41:e12.
[13] Clark LN, Koehler U, Ward DC, Wienberg J, Hewitt JE. Analysis of the organisation and localisation of the FSHD-associated tandem array in primates: implications for the origin and evolution of the 3.3 kb repeat family. Chromosoma 1996; 105:180–9.
[14] Ballarati L, Piccini I, Carbone L, et al. Human genome dispersal and evolution of 4q35 duplications and interspersed LSau repeats. Gene 2002;296:21–7.
[15] Deidda G, Cacurri S, Grisanti P, Vigneti E, Piazzo N, Felicetti L. Physical mapping evidence for a duplicated region on chromosome 10qter showing high homology with the facioscapulohumeral muscular dystrophy locus on chromosome 4qter. Eur J Hum Genet 1995;3:155–67.

[16] van Geel M, Dickson MC, Beck AF, et al. Genomic analysis of human chromosome 10q and 4q telomeres suggests a common origin. Genomics 2002;79:210–7.
[17] Matsumura T, Goto K, Yamanaka G, et al. Chromosome 4q;10q translocations; comparison with different ethnic populations and FSHD patients. BMC Neurol 2002;2:7.
[18] Lemmers RJ, van der Maarel SM, van Deutekom JC, et al. Inter- and intrachromosomal sub-telomeric rearrangements on 4q35: implications for facioscapulohumeral muscular dystrophy (FSHD) aetiology and diagnosis. Hum Mol Genet 1998;7: 1207–14.
[19] Deidda G, Cacurri S, Piazzo N, Felicetti L. Direct detection of 4q35 rearrangements implicated in facioscapulohumeral muscular dystrophy (FSHD). J Med Genet 1996;33:361–5.
[20] Lee JH, Goto K, Matsuda C, Arahata K. Characterization of a tandemly repeated 3.3-kb KpnI unit in the facioscapulohumeral muscular dystrophy (FSHD) gene region on chromosome 4q35. Muscle Nerve 1995;2:S6–S13.

Human Molecular Genetics, 2006, Vol. 15, No. 8 1279–1289
doi:10.1093/hmg/ddl045
Advance Access published on March 10, 2006

Aberrant neuromuscular junctions and delayed terminal muscle fiber maturation in α-dystroglycanopathies

Mariko Taniguchi[1], Hiroki Kurahashi[3], Satoru Noguchi[4], Takayasu Fukudome[5], Takeshi Okinaga[2], Toshifumi Tsukahara[6], Youichi Tajima[7], Keiichi Ozono[2], Ichizo Nishino[4], Ikuya Nonaka[4] and Tatsushi Toda[1,*]

[1]Division of Clinical Genetics, Department of Medical Genetics and [2]Department of Pediatrics, Osaka University Graduate School of Medicine, 2-2 Yamadaoka, Suita, Osaka 565-0871, Japan, [3]Division of Molecular Genetics, Institute for Comprehensive Medical Science, Fujita Health University, Toyoake, Aichi 470-1192, Japan, [4]National Institute of Neuroscience, National Center of Neurology and Psychiatry, Kodaira, Tokyo 187-8502, Japan, [5]Division of Clinical Research, Nagasaki Medical Center of Neurology, Kawatanamachi, Nagasaki 859-3615, Japan, [6]Center for Nano Materials and Technology, Japan Advanced Institute of Science and Technology, Tatsunokuchi, Ishikawa 923-1292, Japan and [7]Department of Clinical Genetics, The Tokyo Metropolitan Institute of Medical Science, Bunkyo-ku, Tokyo 113-8613, Japan

Received October 15, 2005; Revised and Accepted February 28, 2006

Recent studies have revealed an association between post-translational modification of α-dystroglycan (α-DG) and certain congenital muscular dystrophies known as secondary α-dystroglycanopathies (α-DGpathies). Fukuyama-type congenital muscular dystrophy (FCMD) is classified as a secondary α-DGpathy because the responsible gene, *fukutin*, is a putative glycosyltransferase for α-DG. To investigate the pathophysiology of secondary α-DGpathies, we profiled gene expression in skeletal muscle from FCMD patients. cDNA microarray analysis and quantitative real-time polymerase chain reaction showed that expression of developmentally regulated genes, including myosin heavy chain (*MYH*) and myogenic transcription factors (*MRF4*, *myogenin* and *MyoD*), in FCMD muscle fibers is inconsistent with dystrophy and active muscle regeneration, instead more of implicating maturational arrest. FCMD skeletal muscle contained mainly immature type 2C fibers positive for immature-type MYH. These characteristics are distinct from Duchenne muscular dystrophy, suggesting that another mechanism in addition to dystrophy accounts for the FCMD skeletal muscle lesion. Immunohistochemical analysis revealed morphologically aberrant neuromuscular junctions (NMJs) lacking MRF4 co-localization. Hypoglycosylated α-DG indicated a lack of aggregation, and acetylcholine receptor (AChR) clustering was compromised in FCMD and the myodystrophy mouse, another model of secondary α-DGpathy. Electron microscopy showed aberrant NMJs and neural terminals, as well as myotubes with maturational defects. Functional analysis of NMJs of α-DGpathy showed decreased miniature endplate potential and higher sensitivities to *d*-Tubocurarine, suggesting aberrant or collapsed formation of NMJs. Because α-DG aggregation and subsequent clustering of AChR are crucial for NMJ formation, hypoglycosylation of α-DG results in aberrant NMJ formation and delayed muscle terminal maturation in secondary α-DGpathies. Although severe necrotic degeneration or wasting of skeletal muscle fibers is the main cause of congenital muscular dystrophies, maturational delay of muscle fibers also underlies the etiology of secondary α-DGpathies.

* To whom correspondence should be addressed. Tel: +81 668793380; Fax: +81 668793389; Email: toda@clgene.med.osaka-u.ac.jp

INTRODUCTION

Fukuyama-type congenital muscular dystrophy (FCMD; MIM 253800) is an autosomal recessive muscular dystrophy and the second most common childhood muscular dystrophy in Japan, following Duchenne muscular dystrophy (DMD) (1). Clinical manifestations of FCMD include severe congenital muscular dystrophy from early infancy, cobblestone lissencephaly and eye malformation. We previously isolated the responsible gene for FCMD, termed *fukutin* (2,3). Recently, it has been postulated that *fukutin* modulates the glycosylation of α-dystroglycan (α-DG), a major component of the dystrophin–glycoprotein complex (4,5). FCMD is classified as one of the congenital muscular dystrophies, such as laminin-α2-deficient congenital muscular dystrophy (MDC1A) (6). Recently, FCMD has also been classified as a secondary α-DGpathy, as mutations in genes encoding glycosyltransferases result in hypoglycosylated α-DG (7). α-Dystroglycan binds to extracellular matrix proteins such as laminin, agrin and perlecan, which are important in maintaining muscle cell integrity (8). Hypoglycosylated α-DG provokes the post-translational disruption of dystroglycan–ligand interactions in the skeletal muscle of patients, leading to the severe phenotypes of congenital muscular dystrophies (7). Other glycosyltransferases include POMGnT1 (protein *O*-mannose β-1, 2-*N*-acetylglucosaminyltransferase 1), POMT1 and POMT2 (protein *O*-mannosyltransferases 1 and 2), fukutin-related protein (FKRP) and LARGE; mutations in these genes induce human muscle–eye–brain disease, Walker–Warburg syndrome and congenital muscular dystrophy type 1C/1D, and mouse myodystrophy, respectively (9–14).

Primary characteristics of the so-called 'muscular dystrophy' such as DMD include necrotic change and active regeneration of muscle fibers. From infancy, DMD patients usually show dystrophic change in skeletal muscle, accompanied by elevation of serum creatine kinase (CK) levels. However, DMD patients usually maintain their gait until early adolescence. In contrast, FCMD patients show severe phenotypic characteristics from very early infancy, and few patients can acquire gait regardless of serum CK levels (1). Skeletal muscle fibers in FCMD are extremely small, irregular in cell size and architecturally disorganized, and extensive fibrosis prevails from the early infantile stage. However, only a small number of muscle fibers show severe necrotic change or active myofibril regeneration, and satellite cells are also fewer than those of DMD (1,15,16). These phenotypic differences promote the hypothesis that another mechanism may also account for the pathophysiology of secondary α-DGpathies.

Although expression profiling of skeletal muscle from patients with DMD, MDC1A and α-sarcoglycanopathy have been described (17–19), no similar analysis has been reported for FCMD and other secondary α-DGpathies. To investigate the molecular mechanism of FCMD and other secondary α-DGpathies, we profiled gene expression in FCMD skeletal muscle using cDNA microarray and subsequent quantitative real time polymerase chain reaction (PCR). Here we demonstrate that aberrant neuromuscular junctions (NMJs) and maturational delay of muscle fibers are significant to the mechanism underlying secondary α-DGpathies.

RESULTS

Aberrant muscle regeneration is suggested by gene expression profiling of FCMD skeletal muscle

Gene expression profiling of FCMD skeletal muscle was performed using a custom cDNA microarray. Clustering analysis showed similar overall expression profiles of muscle from four FCMD patients, aged 20 days to 1 year, 6 months (Fig. 1A). This similarity is independent of age and histology of the muscle specimen in our samples.

We analyzed individual genes showing distinct expression patterns in FCMD skeletal muscle compared with normal children or DMD patients. Most genes encoding muscle components were down-regulated in FCMD. Among these, *myosin light chain 1, 3* and *4* (*myl1, 3* and *4*) were up-regulated in DMD skeletal muscle, in contrast with FCMD (Fig. 1B). Expression of the developmentally regulated myosin heavy chains (*MYHs*), *MYH1*, *MYH2* and *MYH7* (slow, adult-type), was down-regulated in FCMD but not in DMD, whereas expression of *MYH8* (fast-type) showed no significant change in FCMD compared with DMD or normal controls. Slow-type MYHs (MYH1, MYH2 and MYH7) are present in mature muscle fibers and crucial for sarcomere assembly to maintain muscle integrity, whereas fast-type or developmental MYHs (MYH3, MYH4 and MYH8) are seen in early immature myoblasts or in regenerating fibers. These observations suggest that expression of mature muscle components is suppressed in FCMD skeletal muscle at all ages examined.

With regard to muscle fiber differentiation, myogenic factors including *MyoD*, *myf5* and *myogenin* (*myf4*) showed insufficient signal for the analysis. It is noteworthy, however, that *MRF4* (*myf6*) was down-regulated in FCMD. Expression of the alpha-type cholinergic receptor (*CHRNA*), which is known to be regulated by *MyoD* and *MRF4* (20,21), was much higher in FCMD patients than in normal controls.

We next performed real-time quantitative PCR to further investigate skeletal muscle differentiation. We compared mRNA expression in FCMD muscle with normal or DMD skeletal muscle, as DMD is a good example for active regeneration, in which expression of muscle component and myogenic factor mRNA expression is expected to be up-regulated. Although *CHNRA* was up-regulated in DMD, as predicted, its expression was even higher in FCMD (Fig. 2A and B). Among these cholinergic receptor subtypes, gamma-type cholinergic receptor (*CHNRG*), which is a component of fetal isoforms, was up-regulated, whereas epsilon-type cholinergic receptor (*CHNRE*), which only composes adult isoforms (22), was down-regulated in FCMD (Fig. 2B). MYH slow-type (*MYH7*) was down-regulated in FCMD, consistent with the microarray analysis, whereas expression of fast-type MYH (*MYH11b*) was not altered in FCMD. Interestingly, although *MyoD* and *myogenin* were up-regulated in both DMD and FCMD, *MRF4* was down-regulated in FCMD muscle but up-regulated in DMD (Fig. 2A and B). *MRF4* expression is known to be up-regulated in the late phase of muscle regeneration or differentiation, followed by sequential expression of *MyoD*, *myf5* and *myogenin*, indicating significant roles in terminal differentiation (20,21). These results suggest that FCMD skeletal muscle undergoes an unbalanced differentiation process.

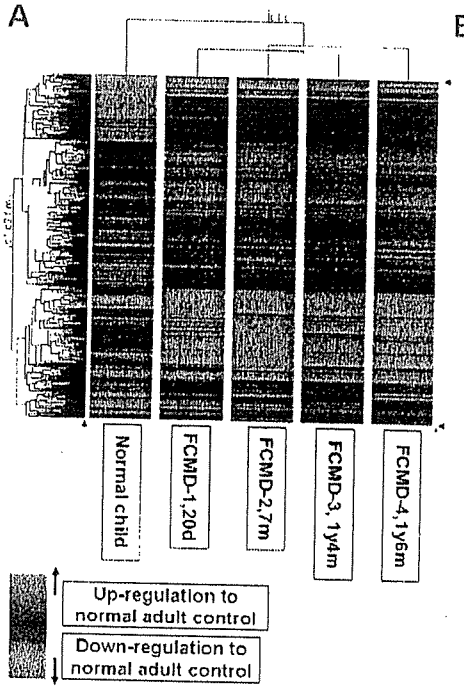

B

gene	FCMD	DMD	Product
myl1	↓	→	myosin light chain 1
myl2	↓	↑	myosin light chain 2
myl3	↓	↑	myosin light chain 3
myl4	↓	↑	atrial /embryonic alkali myosin light chain
myh1	↓↓	↑	myosin, heavy polypeptide 1, adult (slow)
myh2	↓↓	↑	myosin, heavy polypeptide 2, adult (slow)
myh7	↓↓	↑	myosin, heavy polypeptide 7, beta (slow)
myh8	↓	→	myosin, heavy polypeptide 8, (fast)
mybpc1	↓↓	↑	myosin binding protein C, slow type
mybph	↑	→	myosin-binding protein H
actc	↑	↑	actin, alpha, cardiac muscle precursor
actg1	↓	↑	actin, gamma 1
actg2	↓	↑↑	actin, gamma 2
sgcb	↓↓	↓	sarcoglycan, beta
tcap	↓↓	→	titin-cap (telethonin)
ttn	↓↓	↓	titin
des	↓↓	↑	desmin
myf6	↓	→	MRF4 (myf6,herculin)
CHRNA	↑↑	→	nicotinic type, acetylcholine receptor

Figure 1. Cluster image and gene trees from expression profiling of FCMD and normal skeletal muscle. (A) Each line corresponds to the expression signal of each gene. Genes are ordered using the average linkage clustering method to group similar expression profiles. Red denotes up-regulated genes and green denotes down-regulated genes compared with adult control muscle. Note that the expression trends are almost identical within FCMD patients, and FCMD trends are distinct from those of normal children. (B) Expression profile of major muscle components of FCMD and DMD compared with that of normal children. Arrows show the relative expression change (single upward arrow and downward arrow, more than 2-fold increase/decrease; double upward arrows and downward arrows, more than 10-fold increase/decrease; rightward arrow, no change). Note that majority of muscle components are down-regulated in FCMD muscles.

Final maturation step is retarded in FCMD skeletal muscle

To investigate how differentiation is impaired, we examined histological specimens of FCMD skeletal muscle. Marked interstitial tissues with numerous small, round-shaped immature fibers and some necrotic fibers increased with age were seen in FCMD skeletal muscle specimens. Interstitial tissue is prominent from early infancy and progresses with age (Fig. 3A–C), and skeletal muscle from an FCMD fetus also shows rich interstitial tissues (Fig. 3E). Although necrotic change in muscle fibers is not so marked as in DMD fibers, DMD muscle shows less marked fibrosis and more mature fibers, despite more active necrotic and regenerating processes (Fig. 3D). Overall, FCMD muscle is reminiscent of fetal muscle: skeletal muscle from a normal fetus appears rich in fibrous tissues and small, round-shaped immature myotubes (Fig. 3F).

Muscle fiber type is easily identified by ATPase staining. Normally, type 2C fibers are mainly seen in fetal muscle fibers or in regenerating fibers. However, in ATPase-stained cryospecimens, FCMD muscle showed a significantly higher percentage of undifferentiated type 2C muscle fiber contents relative to DMD or control samples ($P < 0.005$) (Fig. 3G and H, Table 1).

Using immunohistochemical analysis, we examined MYH subtypes to confirm the differentiation impairment in FCMD and in myodystrophy mouse (*myd*), which is another model of secondary α-DGpathies. In normal muscle from age-matched controls, no staining of developmental or neonatal MYH (Fig. 3I and J) was seen. In contrast, FCMD and *myd* muscle fibers stained positively for developmental and neonatal MYHs (Fig. 3M and N). These positive fibers corresponded with those staining positive for fast-type MYHs in a serial section (Fig. 3M–O, arrows). Similar staining patterns were observed in skeletal muscle from an FCMD fetus. It is unlikely that all fibers showing developmental MYH expression are derived from regenerating fibers, as few active regenerating or necrotic fibers are seen in the hematoxylin and eosin (HE) specimen at any ages (Fig. 3A–C). Similar staining patterns were observed in skeletal muscles from an FCMD fetus and adult *myd* (data not shown). It is unlikely that all fibers showing developmental MYH expression are derived from regenerating fibers, as few active regenerating or necrotic fibers are seen in the HE specimen (Fig. 3A–C).

These results induce the possibility that maturation might be slowed or arrested in FCMD and *myd* skeletal muscles, and possibly this is common in secondary α-DGpathies. It also

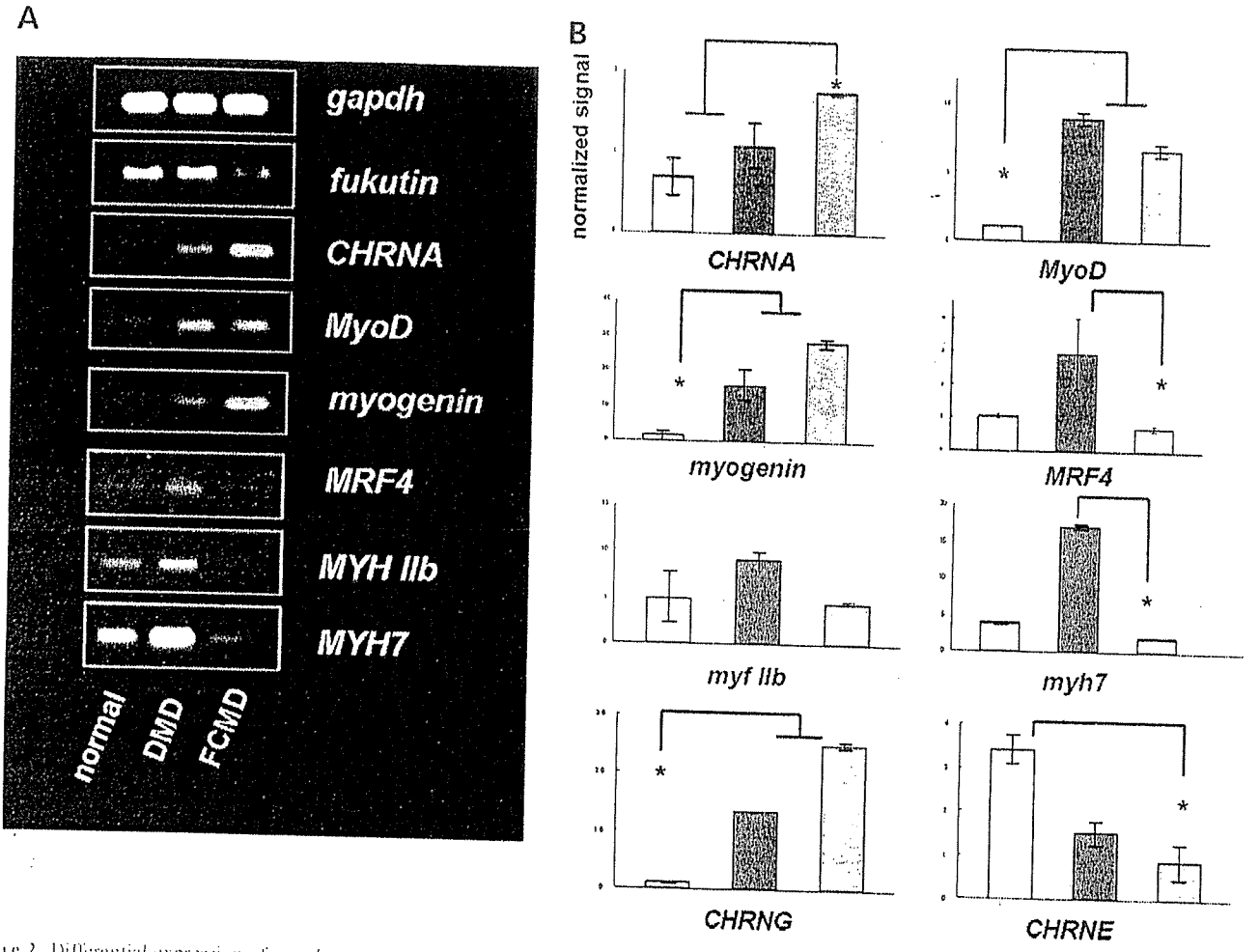

Figure 2. Differential expression of muscle components and myogenic factors in skeletal muscles from FCMD, DMD and normal children. (A) PCR products show that *MyoD* and *myogenin*, which are sequentially expressed in the early phase of muscle regeneration, are up-regulated in DMD and FCMD; however *MYH* and *MRF4* are down-regulated in FCMD but not DMD. (B) Quantitative real-time PCR analysis of mRNA expression. Each bar represents the mean value and 95% confidence interval of duplicate experiments in two patients for each disease and normal control. White bar, normal children; black bar, DMD; gray bar, FCMD. Expression levels are plotted as values normalized to *gapdh*. $^*P < 0.005$ (Student's *t*-test).

implies that secondary α-DGpathies have more complex etiology than the so-called 'muscular dystrophy', and that may be partly explained by a maturational defect.

NMJ abnormalities induce maturational delay in secondary α-DGpathies

Microarray analysis showed a reduction in *MRF4* expression in FCMD. Using immunochemistry, we further investigated MRF4 expression in FCMD and in *myd*. Immunoreactivity against MRF4 was reduced dramatically in FCMD muscle fibers (Fig. 4A). In normal skeletal muscles, anti-MRF4 antibody yielded strong signals, which co-localized with the nucleus and NMJs (Fig. 4A, upper columns). MRF4 in FCMD muscles showed weak signals which were not merged with NMJ (Fig. 4A, lower columns). Similar results were obtained in *myd* (data not shown). Regarding the fact that MRF4 is required at the time and place of NMJ development during skeletal muscle differentiation (23), these results prompt the hypothesis that the differentiation process of muscle fibers arrests at this point in secondary α-DGpathies.

We next examined the morphology of NMJs in both FCMD and *myd* by staining acetylcholine receptor (AchR) in NMJs with anti-α-bungarotoxin (Fig. 4B). Almost all the NMJs of FCMD and *myd* showed sparse, weak staining (Fig. 4B, lower columns), in contrast with the dense pattern in normal skeletal muscle (Fig. 4B, upper columns). In normal skeletal muscles, the borders of positive signals were characteristically flared because of multiple layers of synaptic folds, whereas borders in FCMD and *myd* appear smooth and simple, and synaptic folds—particularly secondary folds—were seldom observed. This signal pattern reflects deteriorated or non-deteriorated cluster of AChR on NMJs in secondary α-DGpathies.

Electron microscopic examination of these secondary α-DGpathies revealed aberrant NMJ lesions with abnormal neural endings. NMJs with fewer synaptic folds and secondary clefts were seen in all NMJs of FCMD and *myd* (Fig. 5A–F). In addition, the muscle fibers showed characteristics of immaturity, consistent with our hypothesis that the myotubes are maturationally arrested (Fig. 5G and H). These fibers are distinct from the active regenerating

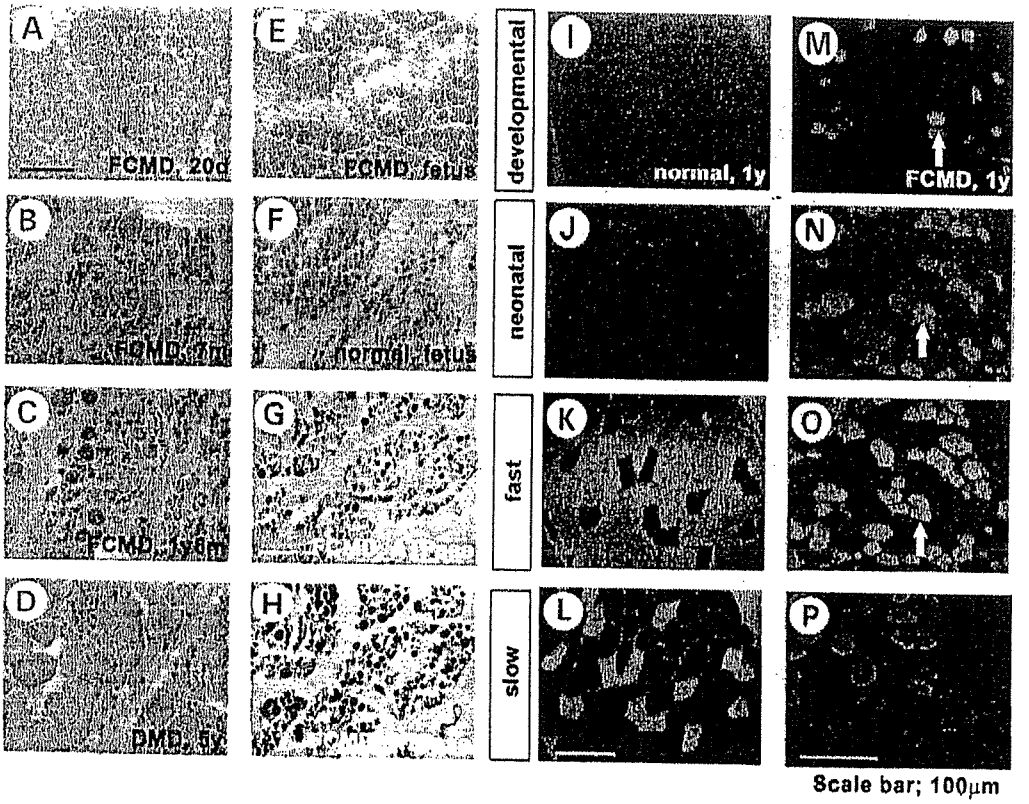

Figure 3. HE and ATPase stains of biopsied FCMD skeletal muscle, used for microarray analysis. Each specimen shows marked fibrosis with numerous small immature muscle fibers, which is seen from early infancy (A, 20 days; B, 7 months; C, 1-year 6 months), and progresses with age. DMD muscle (D, 5 years) shows less marked fibrosis and less frequent immature fibers despite more active necrotic and regenerating processes. Note that the pathological findings of FCMD skeletal muscles are similar to those of fetal skeletal muscles (E, FCMD fetus, 19 weeks; F, normal fetus, 21 weeks). Also note many undifferentiated immature type 2C fibers stained darkly for ATPase under both alkaline (pH 10.4) (G) and acid (pH 4.6) (H) pre-incubations. Immunostaining for MYH subtypes shows positive staining of developmental and neonatal MYH and decreased staining of slow-type MYH, which are distinct from normal muscles (normal child muscles, I year, I–L; FCMD, 1 year, M–P in sequential cryosections). Scale bars = 100 μm.

Table 1. Muscle contents and type 2C fibers in biopsied specimen of FCMD, DMD and normal children

Disease	Age	Muscle (%)	Type 2C (%)	Fibrosis (%)
FCMD (F1)	20 days	71	26	27
FCMD (F2)	7 months	53	26	41
FCMD (F3)	1-year 4 months	60	25	42
FCMD (F4)	1-year 6 months	52	19	43
DMD[a]	3–9 years	61	9	30
Normal[a]	1 year	≥95	≤5	≤5

[a]Average, $n = 10$

myotubes seen in DMD muscle fibers, in that ribosome particles appear quite poor.

We performed functional analysis of the morphologically aberrant NMJs in secondary α-DGpathy by measuring miniature endplate potential (MEPP) and endplate potential (EPP) of *myd* mice (Table 2). The amplitudes of MEPP were markedly lower in *myd* mice than in normal littermates ($P < 0.005$). In contrast, quantal content of EPP was increased in *myd* ($P < 0.005$). The reduction of MEPP amplitude could be compensated by the increased quantal content, and the safety margin of neuromuscular transmission is considered to be maintained in *myd* mice. The number of endplates recorded in *myd* mice was much fewer than in normal littermates. However, the amount of *d*-Tubocurarine that can inhibit the muscle contraction induced by the EPP was distinctively low for *myd* muscle relative to that of normal littermate (Table 2). These findings implicate, combined with the morphological observation, that most of the endplates in *myd* are not adequately innervated, but a small number of NMJs functionally compensate the low MEPP amplitude to maintain the safety margin of neuromuscular transmission.

Hypoglycosylation of α-DG as the etiology of non-clustering AChR in NMJs

We performed immunostaining to examine core α-DG in muscle fibers. In normal skeletal muscles, α-DG localized to the NMJ and sarcoplasmic membrane (Fig. 6A). In contrast, FCMD and *myd* showed substantial α-DG on the sarcoplasmic membrane, but only weak signals were observed in thin NMJs, indicating a failure of α-DG aggregation (Fig. 6A, normal NMJs, arrows; FCMD and *myd*, arrowheads). We also examined staining of glycosylated α-DG (IIH6). As expected, we saw no signal on NMJs or on the sarcoplasmic membrane in FCMD and *myd* (data not shown), implying that glycosylation

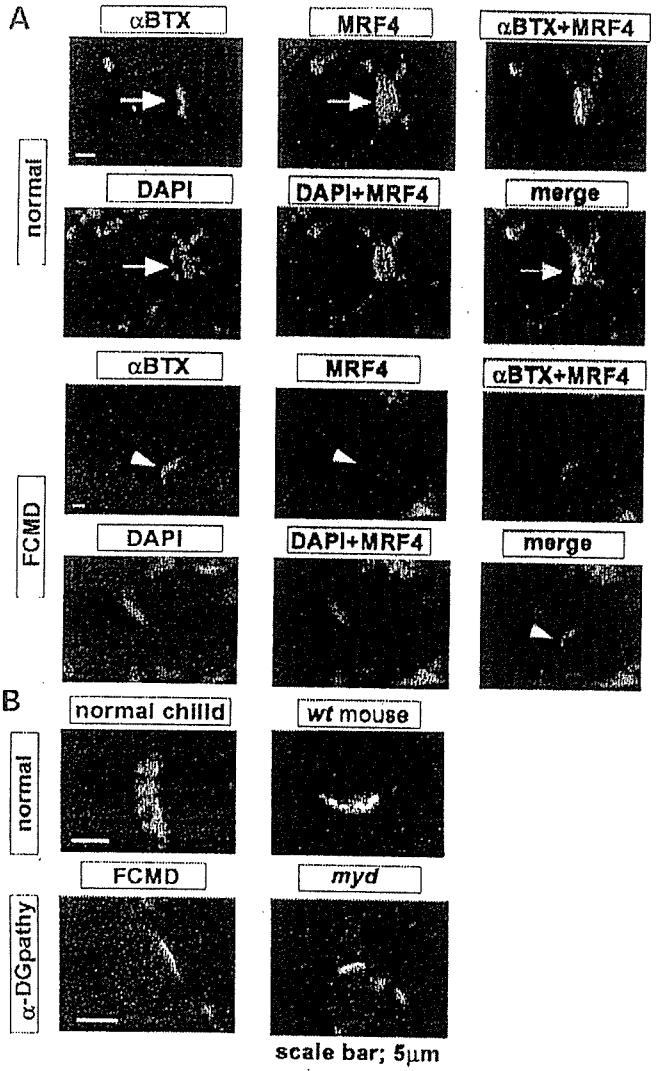

Figure 4. Immunohistochemistry of MRF4 in secondary α-DGpathy and aberrant NMJs in secondary α-DGpathy. (A) Fluorescence image of MRF4 (green), α-bungarotoxin staining of AChR on NMJ (red) and DAPI-stained nuclei (blue) in normal and FCMD skeletal muscles. In normal muscle, NMJs stain strongly, merging with MRF4 staining and DAPI (arrows, upper columns). In FCMD, the staining pattern of MRF4 in the nucleus of muscle fibers is markedly decreased and no merging stain with NMJ is seen (arrowhead). (B) Compared with normal AChR on NMJs (red) stained by α-BTX (upper columns), scattered, fold-less staining pattern is present in both FCMD and *myd* (lower columns). Scale bars = 5 μm.

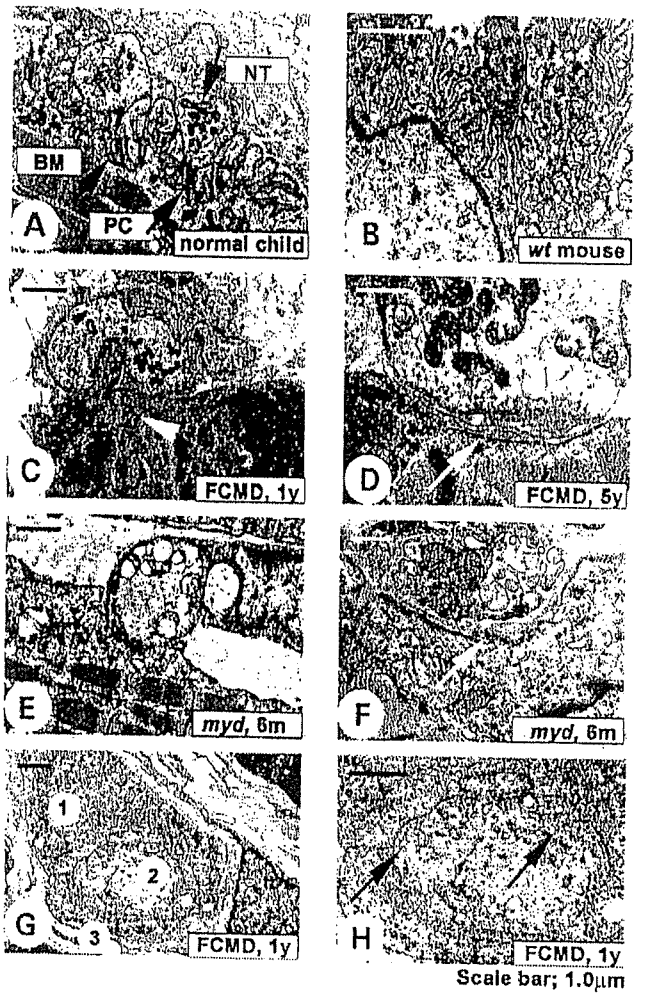

Figure 5. Electron microscopic examinations of NMJs and skeletal muscle from secondary α-DGpathies. Aberrant NMJs and myotubes with maturational arrest are seen in secondary α-DGpathies. Compared with normal (A, human; B, *wt* mouse), NMJs in FCMD (C and D) and *myd* (E and F) show simpler secondary clefts and wider synaptic clefts with occasional multilayered basal lamina (D and F, white arrows). Moreover, maturationally arrested myotubes are seen in secondary α-DGpathy. Three cells (1–3) share a common basement membrane (G), and at higher magnification, these myotubes contain poorly organized myofibrils (black arrows) (H). In contrast with early regenerating fibers in normal regenerating myotubes, ribosome particles are not abundant in FCMD, indicating maturational arrest of myotubes in secondary α-DGpathy. Abbreviation: PC, primary cleft; NT, nerve terminal; BM, basal lamina. Scale bars = 1.0 μm.

is crucial for α-DG aggregation and also for the subsequent clustering of AChR in NMJs. α-DG is expressed on both the muscle peripheral membrane and the peripheral nerve terminal at NMJs (24). Thus, we examined whether a pre-synaptic or post-synaptic lesion contributes to aberrant NMJ formation. Staining for synaptophysin at the pre-synaptic region or for fasciculin at the synaptic gap showed abnormal patterns similar to that of α-bungarotoxin (Fig. 6B). These observations indicate that NMJ abnormalities in secondary α-DGpathies may arise not only at the post-synaptic muscle peripheral membrane, but also by pre-synaptic hypoglycosylated α-DG.

Utrophin and dystrophin are expressed abundantly in pre- and post-synaptic regions of mature NMJs and suggested to play an important role for synaptic maturation and the maintenance of NMJs (25). To analyze aberrations of the distribution of utrophin and dystrophin, we performed immunostaining for utrophin and dystrophin in NMJs. Examination under confocal microscopy allowed a precise view of both proteins on the sarcoplasmic membrane. In NMJs from a normal sample, utrophin strongly stains exclusively at fine primary and secondary synaptic folds, tangled with dystrophin staining just beneath the muscle peripheral membrane (Fig. 6C, left column; Fig. 6D, upper columns). In contrast, NMJs from secondary α-DGpathies show thinner, fold-less and weak signals for both utrophin and dystrophin (Fig. 6C, right column; Fig. 6D, middle and lower